Local buckling and shift of effective centroid of cold-formed steel columns

Ben Young†

Department of Civil Engineering, The University of Hong Kong, Pokfulam Road, Hong Kong

Abstract. Local buckling is a major consideration in the design of thin-walled cold-formed steel sections. The main effect of local buckling in plate elements under longitudinal compressive stresses is to cause a redistribution of the stresses in which the greatest portion of the load is carried near the supporting edges of the plate junctions. The redistribution produces increased stresses near the plate junctions and high bending stresses as a result of plate flexure, leading to ultimate loads below the squash load of the section. In singly symmetric cross-sections, the redistribution of longitudinal stress caused by local buckling also produces a shift of the line of action of internal force (shift of effective centroid). The fundamentally different effects of local buckling on the behaviour of pin-ended and fixed-ended singly symmetric columns lead to inconsistencies in traditional design approaches. The paper describes local buckling and shift of effective centroid of thin-walled cold-formed steel channel columns. Tests of channel columns have been described. The experimental local buckling loads were compared with the theoretical local buckling loads obtained using an elastic finite strip buckling analysis. The shift of the effective centroid was also compared with the shift predicted using the Australian/New Zealand and American specifications for cold-formed steel structures.

Key words: cold-formed steel; columns; effective width; experimental investigation; local buckling; shift of effective centroid; slender sections; structural stability.

1. Introduction

The development and use of cold-formed steel structural members in building construction began in the mid eighteenth century in the United States and Great Britain. However, such structural members were not widely used in the building industry until in the mid nineteenth century where the first edition of the American Iron and Steel Institute Specification for the design of cold-formed steel structural members (AISI 1946) was published.

The use of cold-formed steel structural members has increased rapidly in recent years. Cold-formed members can be used economically in domestic and small industrial building construction and other light gauge structures. As compared to thicker hot-rolled members, cold-formed members provide enhanced strength to weight ratio and ease of construction. The manufacturing process of fabricating cold-formed members usually involves brake-pressing and roll-forming of steel sheets and strips to produce a wide range of cross-section shapes. Cold-formed sections are normally thinner than hot-rolled sections and have a different forming process, and hence, the structural behaviour can be quite different.

---

†Associate Professor, E-mail: young@hku.hk

Cold-formed steel channel columns commonly fail in two distinct modes of buckling, namely, local buckling and overall buckling. Interaction between these two modes may occur in some cases. Both local and overall instability represent common causes of structural failure. Distortional buckling is also one of the modes of failure for some sections. As a consequence, structural instability has become a major research area, where both analytical and experimental investigations have been undertaken to overcome the difficulties of the design of cold-formed steel members. Local buckling plays an important role in the design of slender sections. There is a fundamental difference on the behaviour of pin-ended and fixed-ended locally buckled singly symmetric columns due to the shift of effective centroid.

The purpose of this paper is to describe the local buckling and the shift of effective centroid of thin-walled cold-formed channel columns. The concept of effective width and the effective width equations are also described. The experimental local buckling loads were compared with the theoretical local buckling loads of cold-formed steel channel columns. Local, distortional and overall buckling of the channel columns are presented. The shift of effective centroid of singly and doubly symmetric cross-sections is also described in this paper. The shift of the effective centroid of the channel columns was compared with the shift predicted using the Australian/New Zealand Standard for cold-formed steel structures (Aust/NZ 1996) and the American Iron and Steel Institute Specification for the design of cold-formed steel structural members (AISI 1996).

2. Local buckling

2.1. General

Local buckling involves deformation of the component plate elements of the section, with the plate junctions remaining straight as shown in Fig. 1, and is associated with a half-wavelength which compares with the depth of the section. Fig. 2 shows a plain channel subjected to pure compression. A
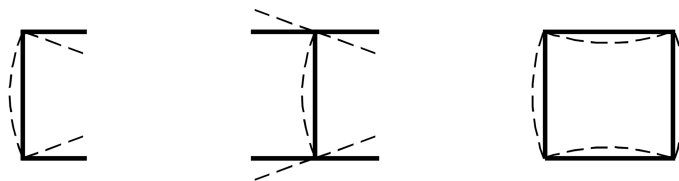

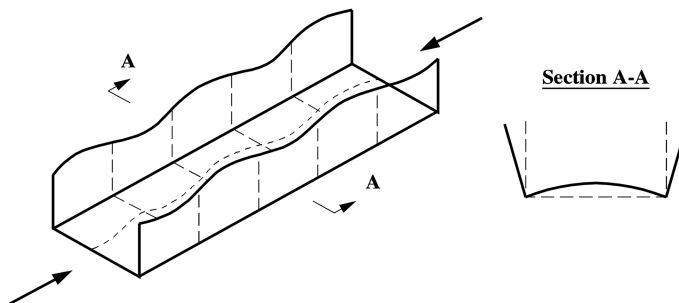Fig. 1 Local buckling modes of typical cross-sections in compression

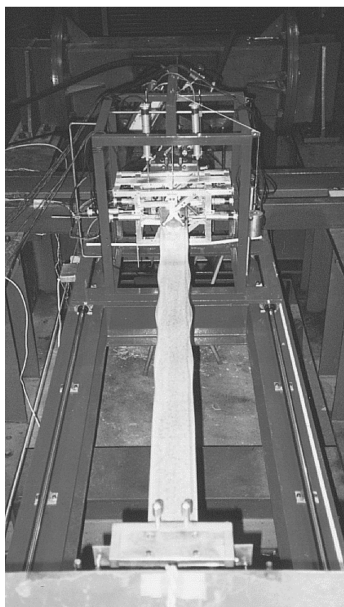Fig. 2 Locally buckled plain channel in compression

Fig. 3 Interaction of local and overall buckling of cold-formed steel plain channel column

photograph of a locally buckled cold-formed plain channel column compressed between fixed ends is shown in Fig. 3. The effect of local buckling plays an important role in the design of slender sections. One of the effects is that it reduces the flexural rigidity of the section and hence the member strength.

2.2. Concept of effective width and effective width equations

A common design procedure to determine the section strength of slender section is to use the concept of effective widths. The concept was first proposed by von Kármán *et al*. (1932). It was introduced following the realization that local buckling of plate elements causes a concentration of the longitudinal stress near the supporting edges of a plate element. A stiffened element is supported longitudinally along two edges, as shown in Fig. 4(a). An unstiffened element is only supported longitudinally along one edge, as shown in Fig. 4(b).
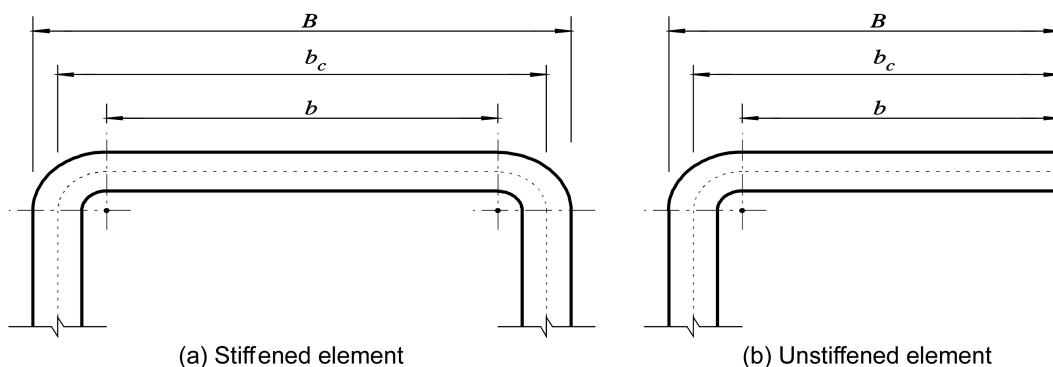

(a) Stiffened element   (b) Unstiffened element

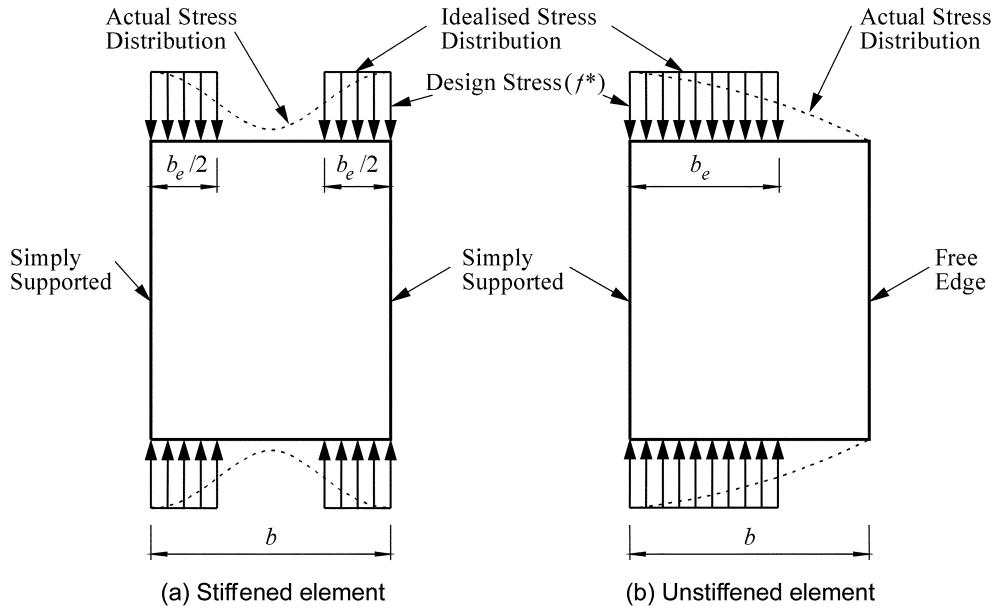Fig. 4 Stiffened and unstiffened elements

Fig. 5 Stress redistribution on uniformly compressed elements after local buckling and effective widths (b_e)

von Kármán suggested that the actual stress distribution at the central portion of a stiffened plate could only support low stress, but the edge portions were capable of supporting high stress. Hence, for uniformly compressed element, the actual stress distribution may be replaced by two effective portions ($b_e/2$) near the supporting edges of a stiffened element, as shown in Fig. 5(a). Similarly, the actual stress distribution may be replaced by one effective portion (b_e) near the supporting edge of an unstiffened element, as shown in Fig. 5(b).

von Kármán *et al.* (1932) proposed the ultimate plate strength (P_u) expression as follows,

$$P_u = b_e t f_y = C\sqrt{Ef_y}t^2 \tag{1}$$

where C is an empirical constant which depends upon the Poisson ratio and the longitudinal support conditions; E is the Young's modulus of elasticity; f_y is the yield stress and t is the plate thickness.

However, the effective width formula by von Kármán is only valid for perfect plates. Geometric imperfections and residual stresses caused by fabrication process exist in real plates. Consequently, it is required to account for the reduction in strength from these imperfections. Winter has proposed and later verified experimentally (1947, 1968) an effective width formula for stiffened compression elements, which based on a series of tests on folded thin-walled sections.

The original formula proposed by Winter is,

$$b_e = 1.9t\sqrt{\frac{E}{f^*}}\left[1 - 0.415\left(\frac{t}{b}\right)\sqrt{\frac{E}{f^*}}\right] \tag{2}$$

which can be rearranged as follows:

$$\frac{b_e}{b} = \sqrt{\frac{p_{cr}}{f^*}}\left[1 - 0.22\sqrt{\frac{p_{cr}}{f^*}}\right] \tag{3}$$

where f^* is the design stress and p_{cr} is the critical elastic buckling stress of a plate. Eq. (3) is called the Winter effective width formula, which is a modification of von Kármán formula. The term within the bracket of Eq. (3) is to account for the effect of imperfections. The equation can be simplified to the following expression,

$$\frac{b_e}{b} = \begin{cases} 1 & \text{when } \lambda \leq 0.673 \\ \dfrac{\left(1 - \dfrac{0.22}{\lambda}\right)}{\lambda} \leq 1.0 & \text{when } \lambda > 0.673 \end{cases} \tag{4}$$

where λ is the slenderness ratio, which is determined as follows,

$$\lambda = \frac{1.052}{\sqrt{K}}\left(\frac{b}{t}\right)\sqrt{\frac{f^*}{E}} \tag{5}$$

where K is the plate buckling coefficient which is a function of the longitudinal edge support conditions. Eq. (4) is widely known and it is used extensively in many cold-formed steel specifications.

2.3. Summary of test program

The test program described in Young (1997), and Young and Rasmussen (1998a, 1998b) provided experimental ultimate loads for cold-formed plain and lipped channel columns compressed between fixed ends and pinned ends. All test specimens were fabricated by brake-pressing from high strength zinc-coated Grade G450 with nominal yield stress of 450 MPa structural steel sheets. The test program comprised four different cross-section geometries. Two series of plain channels and two series of lipped channels were tested, having a nominal thickness of 1.5 mm and a nominal width of the web of 96 mm for all channels. The nominal width of the lip of both lipped channels was 12 mm. The flange width was either 36 mm or 48 mm and was the only variable in the cross-section geometry. Accordingly, the four test series were labelled P36, P48, L36 and L48 where "P" and "L" refer to "plain" and "lipped" channels respectively. The specimens were mainly tested with fixed ends at various column lengths. However, some of the specimens were tested with pinned ends using the same effective lengths as those for the fixed-ended specimens. The shortest specimen lengths complied with the SSRC guidelines (Galambos 1998) for stub column lengths, while the longest produced l_{ey}/r_y ratios of approximately 130, 110, 110 and 100 for Series P36, P48, L36 and L48 respectively, where l_{ey} is the effective length for buckling about the minor y-axis and r_y is the radius of gyration about the y-axis. The measured cross-section dimensions of each set of specimens are detailed in the papers by Young and Rasmussen (1998a, 1998b).

The material properties determined from the coupon tests are summarized in Table 1. The table contains the nominal 0.2% tensile proof stress ($\sigma_{0.2}$), the measured static 0.2% ($\sigma_{0.2}$) and 0.5% ($\sigma_{0.5}$) tensile proof stresses, the tensile strength (σ_u) as well as the Young's modulus (E) and the elongation after fracture (ε) based on a gauge length of 50 mm. The stress-strain curves obtained from the coupon tests are detailed in Young and Rasmussen (1998a, 1998b). Moreover, the details of the residual stress measurements, the local and overall geometric imperfections of the test specimens, and the procedure of the column tests are also given in Young and Rasmussen (1998a, 1998b).

Table 1 Nominal and measured material properties

Test series	Nominal		Measured			
	$\sigma_{0.2}$	E	$\sigma_{0.2}$	$\sigma_{0.5}$	σ_u	ε
	(MPa)	(GPa)	(MPa)	(MPa)	(MPa)	(%)
P36	450	210	550	560	570	10
P48	450	210	510	525	540	11
L36	450	210	515	525	540	11
L48	450	200	550	560	570	10

2.4. Local buckling load

The experimental local buckling loads (N_{lExp}) of the Series P36 and P48 specimens under uniform compression were determined for all fixed-ended tests, except for the long specimens whose ultimate loads were lower than the elastic local buckling load of the column. The experimental local buckling load (N_{lExp}) was determined by plotting the load (N) against the square of a local buckling deformation and subsequently fitting a line through the test points in the post local buckling region. The intercept with the load axis resulting from the line fitted in this region was assumed to be the experimental buckling load (Venkataramaiah and Roorda 1982). The larger of the web deformation and the average of the deformations at the free edge of the flanges at mid-length was used for the plots. The mean and the standard deviation (S.D.) of the experimental local buckling loads for all specimens of each series are given in Table 2.

The theoretical elastic local buckle half-wavelength (l) and the elastic local buckling load (N_{lTh}) were obtained using a finite strip buckling analysis (Hancock 1978). The results are also given in Table 2. The average measured cross-section dimensions of the fixed-ended specimens for each series as well as the measured values of the base metal thickness and the Young's modulus were used to determine the theoretical results. It follows from the table that the mean ratio of the experimental local buckling load to the theoretical local buckling load (N_{lExp}/N_{lTh}) was 1.00 and 0.98 for Series P36 and P48 respectively and that the standard deviations (S.D.) of the same ratios were 0.01 and 0.00 respectively. The theoretical and the experimental local buckling loads were very close, with a maximum difference of 0.7 kN (1.6%) and 0.5 kN (1.4%) for Series P36 and P48 respectively. This result indicates that the finite strip buckling analysis was in excellent agreement with the experimental local buckling loads.

Table 2 Experimental and theoretical local buckling loads

Test series	Experimental		Theoretical		Comparison	
	N_{lExp}		N_{lTh} (kN)	l (mm)	N_{lExp}/N_{lTh}	
	Mean (kN)	S.D.			Mean	S.D.
P36	43.4	0.36	43.6	110	1.00	0.01
P48	35.4	0.17	36.1	130	0.98	0.00

Note: 1 kip=4.45 kN; S.D.=Standard Deviation.

3. Buckling modes for compression members

In designing cold-formed steel compression members, it is important to recognize the different buckling modes. Four buckling modes were encountered in the tests:

- Local buckling
- Distortional buckling
- Overall flexural buckling
- Overall flexural-torsional buckling

A finite strip buckling analysis was used to investigate the possible buckling modes for Series P36, P48, L36 and L48. The computer program THIN-WALL (Papangelis and Hancock 1995) was used to generate plots of buckling stress versus buckle half-wavelength, as shown in Figs. 6(a), 6(b), 6(c) and 6(d) for Series P36, P48, L36 and L48 respectively. The average values of the measured cross-section dimensions of the fixed-ended test specimens and the measured material properties were used in the analysis. The corner radii (r_i) were negligible as a result of the brake-pressing fabrication procedure and were not modelled in the analysis. Residual stresses were also ignored.
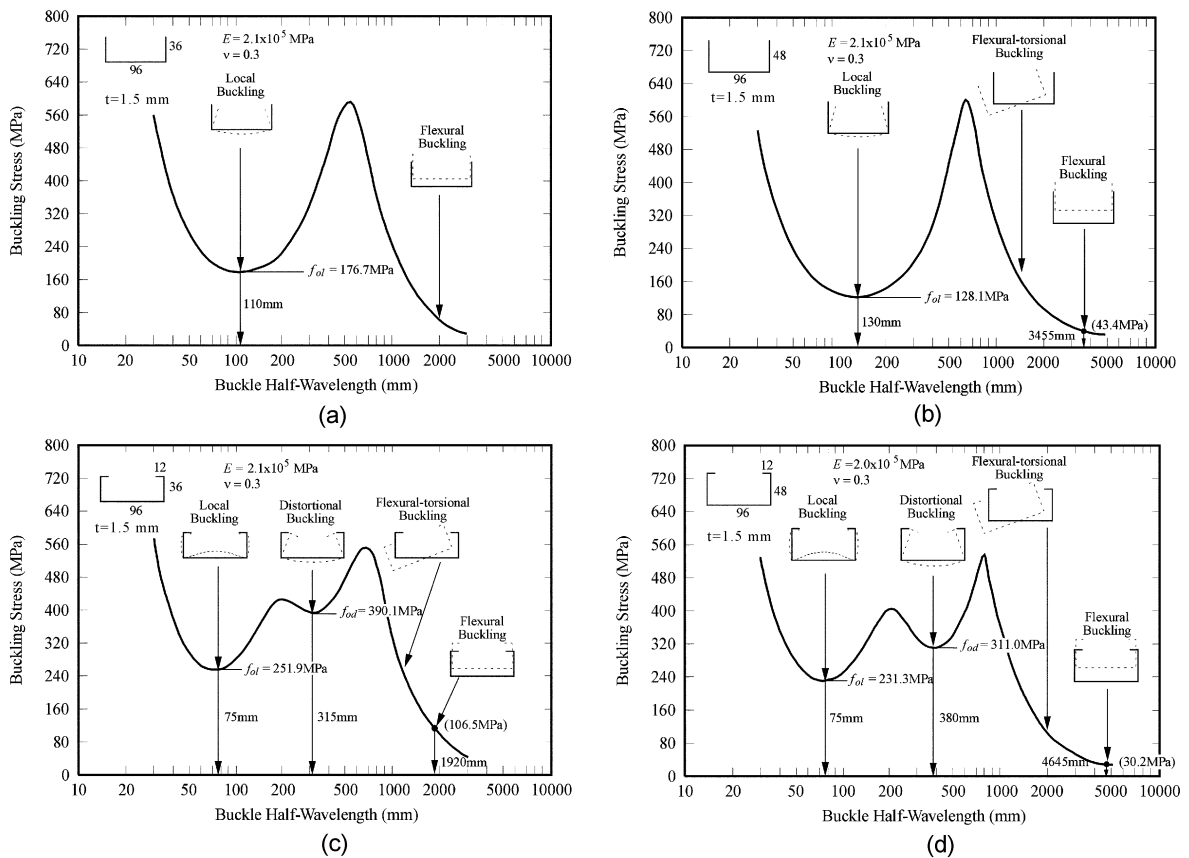

Fig. 6 (a) Finite strip buckling analysis for compression member of Series P36, (b) Finite strip buckling analysis for compression member of Series P48, (c) Finite strip buckling analysis for compression member of Series L36, (d) Finite strip buckling analysis for compression member of Series L48

In the buckling analysis, the plain and the lipped channels were subjected to uniform compression. For the plain channels, the minimum local buckling stresses of 176.7 MPa and 128.1 MPa occurred at half-wavelengths of 110 mm and 130 mm corresponding for Series P36 and P48 respectively, as shown in Figs. 6(a) and 6(b). At long half-wavelengths, flexural-torsional buckling occurred up to 3455 mm, corresponding to a buckling stress of 43.4 MPa, beyond which flexural buckling occurred, as shown in Fig. 6(b) for Series P48. Flexural buckling always occurred at long half-wavelengths for Series P36, as shown in Fig. 6(a).

The results of the buckling analysis of the lipped channels in Series L36 are shown in Fig. 6(c). The local buckling stress of 251.9 MPa and the distortional buckling stress of 390.1 MPa occurred at half-wavelengths of 75 mm and 315 mm respectively. Due to the local buckling stress was lower than the distortional buckling stress, the lipped channel section was likely to undergo local buckling before distortional buckling at intermediate column lengths. At long half-wavelengths, flexural-torsional buckling occurred up to 1920 mm corresponding to a buckling stress of 106.5 MPa, beyond which flexural buckling occurred. The results for Series L48 (which had wider flanges than those in Series L36) followed a similar trend, the local buckling stress of 231.3 MPa and the distortional buckling stress of 311.0 MPa occurred at half-wavelengths of 75 mm and 380 mm respectively. At long half-wavelengths, flexural-torsional buckling occurred up to column length of 4645 mm, corresponding to a buckling stress of 30.2 MPa, beyond which flexural buckling occurred.

4. Shift of effective centroid

4.1. General

The fundamentally different effects of local buckling on the behaviour of pin-ended and fixed-ended singly symmetric columns lead to *inconsistencies in traditional design approaches*. In many codes of practice for cold-formed steel structures, full or partial rotational end restraints are accounted for solely by using certain effective lengths. Furthermore, the design strength of singly symmetric columns is reduced irrespective of the end support conditions in order to account for bending induced in pin-ended columns by the shift of the line of action of the internal force (shift of effective centroid). This procedure is not rational for fixed-ended singly symmetric columns, which may remain straight after local buckling.

4.2. Singly symmetric cross-section

Cold-formed steel members are cold-rolled or brake-pressed into structural shapes. As a result, open cold-formed sections are usually singly-, point- or non-symmetric. The most common types of cross-sections are singly-symmetric plain and lipped channels as well as point-symmetric plain and lipped Z-sections. The boundary conditions for singly symmetric columns are important in the design of thin-walled columns. Local buckling of singly symmetric columns, such as channel sections, may cause overall bending of the column depending on whether the section is compressed between pinned or fixed ends. A uniformly compressed channel section undergoes a shift in the line of action of the internal force when the section locally buckles, as demonstrated in Fig. 7. Rhodes and Harvey (1977) explained that the shift results from the asymmetric redistribution of longitudinal stresses following the development of local buckling deformations, and leads to an eccentricity of the applied load in pin-
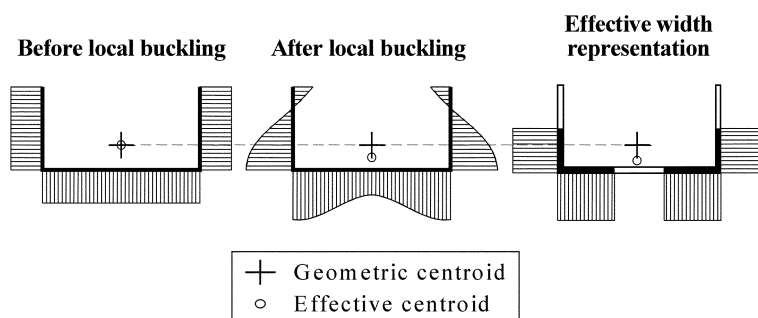
Fig. 7 Stress redistribution of singly symmetric section under uniform compression with effective width representation
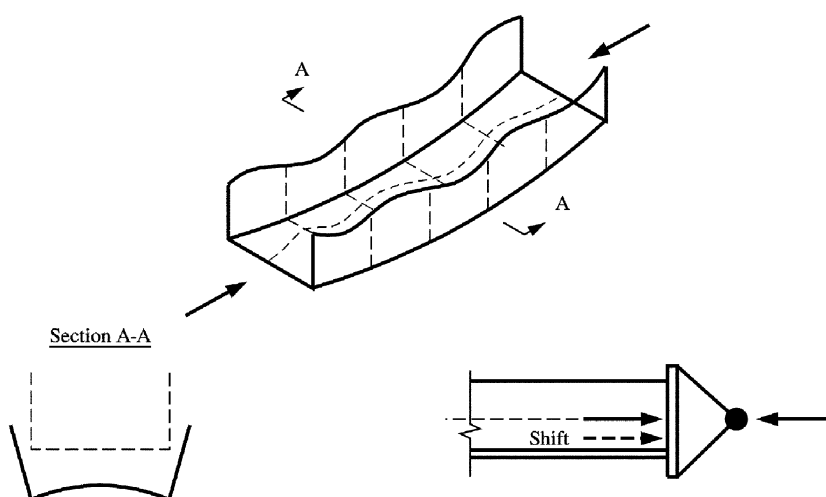

Fig. 8 Locally buckled pin-ended channel column

ended channels. Hence, local buckling of pin-ended channel columns induces overall bending, as shown in Fig. 8. However, this phenomenon does not occur in fixed-ended channel columns as showed by analytical studies (Rasmussen and Hancock 1993) and experimental investigations (Young and Rasmussen 1999a). In this case, the shift in the line of action of the internal force is balanced by a shift in the line of action of the external force, and consequently local buckling does not induce overall bending, as shown in Fig. 9. Thus, the behaviour of pin-ended and fixed-ended singly symmetric columns is fundamentally different.

4.3. Doubly symmetric cross-section

In locally buckled doubly symmetric columns, the redistribution of longitudinal stresses does not cause a shift in the line of action of the internal force because of the section symmetry, as shown in Fig. 10. Therefore, local buckling of doubly symmetric columns does not induce overall bending, regardless of the support conditions. Therefore, the behaviour of locally buckled singly symmetric columns with fixed ends is similar to that of locally buckled doubly symmetric columns with either fixed or pinned ends.
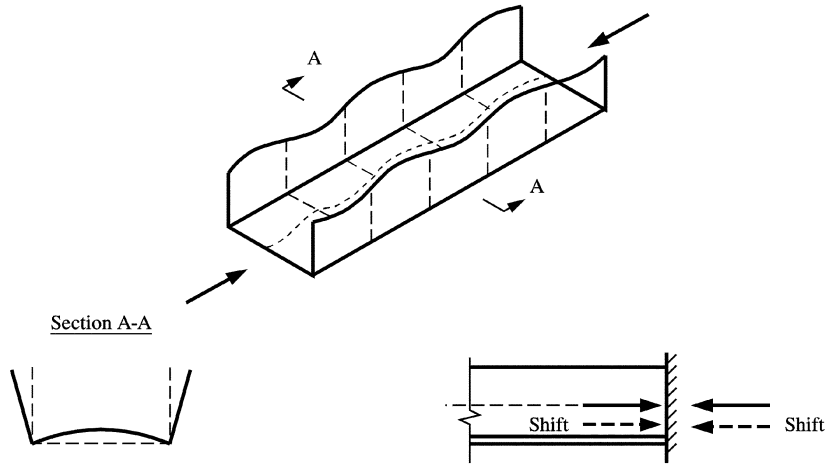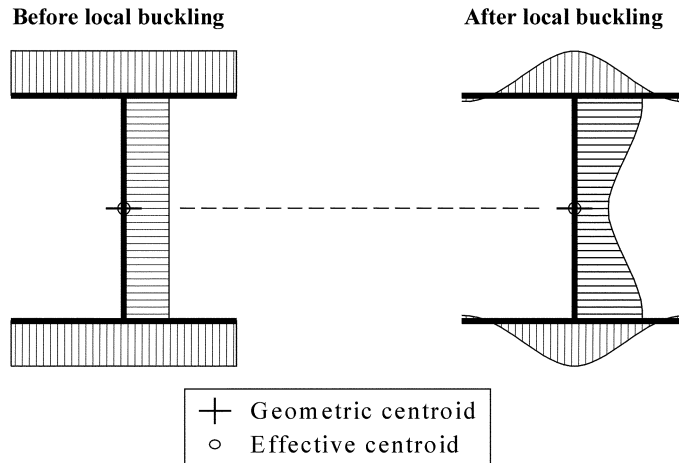
Fig. 9 Locally buckled fixed-ended channel column

Fig. 10 Stress redistribution of doubly symmetric section under uniform compression

4.4. Measurement of shift of effective centroid

The shift of the effective centroid of channel columns has been experimentally investigated by Young and Rasmussen (1999b). Special fixed-ended bearings were used to measure the shift of the effective centroid of the channel column of Series L48 having a column length of 1000 mm. The details of the fixed-ended bearings are given in Young and Rasmussen (2003). The experimental shift (e_S) of the line of action of the applied load (N), is calculated as the ratio of the measured minor axis end moment divided by the measured applied load is shown in Fig. 11. The experimental shift is compared to that predicted using the Australian/New Zealand Standard (Aust/NZ 1996) and the American Iron and Steel Institute Specification (AISI 1996). It follows that the predicted shift is initially towards the lip (positive values of e_S) but changes at a load of approximately 52 kN to shift towards the web, contrary to the measured shift. At the ultimate load, the measured shift is 2.7 mm toward the lips, while the predicted shift is 2.0 mm toward the web.
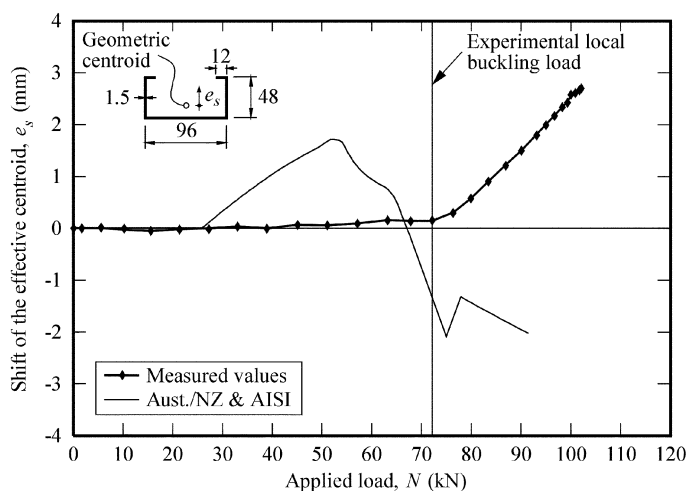
Fig. 11 Shift of effective centroid versus applied load for channel column of Series L48

Young and Rasmussen (1998b) showed that the inaccuracy of the predicted shift led to abnormalities in the design strength curves for lipped channel columns. Young and Rasmussen (1999b) proposed simple modifications to the effective width design rules in the American Iron and Steel Institute Specification (AISI 1996). The proposed effective width design rules provide good agreement between the experimental and the predicted shifts of the effective centroid for lipped channels. The modifications are shown to produce more accurate design strengths for lipped channel columns.

5. Conclusions

The local buckling and the shift of effective centroid of cold-formed steel channel columns have been described. The concept of effective width as well as the von Kármán and the Winter effective width equations have also been described. The experimental local buckling loads of cold-formed steel channel columns were compared with the theoretical local buckling loads obtained using an elastic finite strip buckling analysis. It is shown that the local buckling loads predicted by the finite strip buckling analysis are in excellent agreement with the experimental local buckling loads. Furthermore, the local, distortional and overall buckling stresses and the corresponding half-wavelengths of the channel columns have been presented. The shift of the effective centroid of the cold-formed steel channel columns was compared with the shift predicted using the Australian/New Zealand and the American specifications for cold-formed steel structures.

References

AISI. (1946), *Specification for the Design of Light Gauge Steel Structural Members*, American Iron and Steel Institute, New York.
AISI. (1996), *Specification for the Design of Cold-Formed Steel Structural Members*, American Iron and Steel Institute, Washington, DC.

Aust/NZ. (1996), *Cold-formed Steel Structures*, Australian/New Zealand Standard, AS/NZS 4600:1996, Standards Australia, Sydney, Australia.

Galambos, T.V. (1998), *Guide to Stability Design Criteria for Metal Structures*, 5th Edition, John Wiley & Sons Inc., New York.

Hancock, G.J. (1978), "Local, distortional and lateral buckling of I-beams", *J. Struct. Div.*, ASCE, **104**(11), 1787-1798.

Papangelis, J.P. and Hancock, G.J. (1995), "Computer analysis of thin-walled structural members", *Comput. Struct.*, **56**(1), 157-176.

Rasmussen, K.J.R. and Hancock, G.J. (1993), "The flexural behaviour of fixed-ended channel section columns", *Thin-Walled Structures*, **17**(1), 45-63.

Rhodes, J. and Harvey, J.M. (1977), "Interaction behaviour of plain channel columns under concentric or eccentric loading", *Proc. of the Second Int. Colloquium on the Stability of Steel Structures*, Liege, 439-444.

Venkataramaiah, K.R. and Roorda, J. (1982), "Analysis of local plate buckling experimental data", *Proc. of the Sixth Int. Specialty Conf. on Cold-Formed Steel Structures*, St. Louis, Missouri, 45-74.

von Kármán, T., Sechler, E.E. and Donnell, L.H. (1932), "The strength of thin plates in compression", *Transactions, Applied Mechanics Division,* ASME, **54**, APM-54-5, 53-57.

Winter, G. (1947), "Strength of thin steel compression flanges", *Transactions*, ASCE, **112**, 527-554.

Winter, G. (1968), "Thin-walled structures – Theoretical solutions and test results", *Preliminary Publications of the Eighth Congress, International Association for Bridge and Structural Engineering (IABSE)*, 101-112.

Young, B. (1997), "The behaviour and design of cold-formed channel columns", PhD Thesis, Vol. 1 & 2, Department of Civil Engineering, University of Sydney, Australia.

Young, B. and Rasmussen, K.J.R. (1998a), "Tests of fixed-ended plain channel columns", *J. Struct. Eng.*, ASCE, **124**(2), 131-139.

Young, B. and Rasmussen, K.J.R. (1998b), "Design of lipped channel columns", *J. Struct. Eng.*, ASCE, **124**(2), 140-148.

Young, B. and Rasmussen, K.J.R. (1999a), "Behaviour of cold-formed singly symmetric columns", *Thin-Walled Structures*, **33**(2), 83-102.

Young, B. and Rasmussen, K.J.R. (1999b), "Shift of effective centroid of channel columns", *J. Struct. Eng.*, ASCE, **125**(5), 524-531.

Young, B. and Rasmussen, K.J.R. (2003), "Measurement techniques in the testing of thin-walled structural members", *Experimental Mechanics*, **43**(1), 32-38.

KC